

An Improved Non-linear Weights for Seventh-Order WENO Scheme

Samala Rathan*, G Naga Raju †

Department of Mathematics, Visvesvaraya National Institute of Technology, Nagpur, India

Abstract

In this article, the construction and implementation of a seventh order weighted essentially non-oscillatory scheme is reported for hyperbolic conservation laws. Local smoothness indicators are constructed based on L_1 -norm, where a higher order interpolation polynomial is used with each derivative being approximated to the fourth order of accuracy with respect to the evaluation point. The global smoothness indicator so constructed ensures the scheme achieves the desired order of accuracy. The scheme is reviewed in the presence of critical points and verified the numerical accuracy, convergence with the help of linear scalar test cases. Further, the scheme is implemented to non-linear scalar and system of equations in one and two dimensions. As the formulation is based on method of lines, to move forward in time linear strong-stability-preserving Runge-Kutta scheme (*lSSPRK*) for the linear problems and the fourth order nonlinear version of five stage strong stability preserving Runge-Kutta scheme (*SSPRK*(5, 4)) for nonlinear problems is used.

Keywords: Hyperbolic conservation laws, non-linear weights, smoothness indicators, WENO scheme, *lSSPRK* Runge-Kutta schemes.

MSC: 65M20, 65N06, 41A10.

1 Introduction

The hyperbolic conservation laws arise in many applications such as in gas dynamics, magneto-hydrodynamics (MHD) and shallow water flows. It is well known that even if the initial conditions are smooth, the hyperbolic conservation laws may develop discontinuities in its solution, such as shocks, contact discontinuities etc. Godunov [9] was first to propose a first order upwind scheme for the solution of these equations in the year 1959, which turned out to be a stepping stone for the development of various upwind schemes in the following years. In order to construct a higher order scheme Harten [12, 13] introduced the concept of Total Variation Diminishing (TVD), which says that the total variation to the approximation of numerical solution must be non-increasing with time. Later it was shown that the TVD schemes are having at most of first-order accuracy near smooth extrema [23] .

Harten et al. [14, 15, 16] derived the higher order schemes with the property of relaxing the TVD condition and allowing the occurrence of spurious oscillations in the numerical scheme

*Email: rathan.maths@gmail.com

†Email: gnagaraju@mth.vnit.ac.in

but the $O(1)$ Gibbs-like phenomena is essentially prevented, which is termed as Essentially Non-oscillatory (ENO) property and the schemes are known as ENO schemes. These are the first successful higher order schemes for the spatial discretization of the hyperbolic conservation laws, in a finite-volume formulation. The ENO schemes adopts a strategy of choosing the interpolation points over a stencil which avoids the induction of oscillations in the numerical solution through a smoothness indicator of a solution. And based on this idea the smoothest stencil is chosen from a set of candidate stencils. As a result, the ENO scheme obtains information from smooth regions and avoids spurious oscillations near discontinuities. Further, these schemes were studied in a finite-difference environment by Shu and Osher [31, 32].

The weighted ENO (WENO) schemes are set forth by Liu et al. [22], in a finite-volume frame of reference up to third-order of accuracy. Later, Jiang and Shu [19] have put forward these WENO schemes in a finite-difference setup to a higher order accuracy with the new smoothness indicators. These smoothness indicators are measured in the scaled L_2 norm, that is, they are the sum of the normalized squares, of all derivatives of the local interpolating polynomials. This scheme is referred as WENO-JS in the content to follow. For more details on ENO and WENO schemes, one can refer to the articles [29] and [30]. A very high order schemes are constructed in a similar manner of WENO-JS in [2], which we mention them here as WENO-BS schemes. Seventh order WENO-BS scheme is revised in [27, 28] and inspected the scheme in the presence of critical points.

Henrick et al. [17] examined that the actual convergence rate of the fifth-order WENO-JS scheme is less than the desired order, for the problems where the first and third order derivatives of the flux do not vanish simultaneously. In addition, it was ascertained that the convergence rate of the scheme is sensitive to the parameter ϵ , employed in the evaluation of smoothness indicators to overcome from vanishing denominator. The authors revived the WENO-JS scheme by using a mapping function on the nonlinear weights such that the scheme, named as mapped WENO, satisfies the sufficient condition where WENO-JS fails and achieves an optimal order of convergence near simple smooth extrema. Subsequently, a very high order WENO schemes were developed based on the mapping function in [8].

Borges et al. [3] reviewed the fifth-order WENO schemes, entitled as WENO-Z scheme, by initiating a global smoothness indicator, which measures the smoothness of the larger stencil utilized in the construction of nonlinear weights. It was numerically validated that WENO-Z scheme is less dissipative than WENO-JS scheme and more efficient than mapped WENO scheme. WENO-Z scheme retained the convergence order as four at the first-order critical points, degrade to two when higher order critical points are encountered. These thoughts are extended by Castro et al. [4] to higher order schemes and produced a closed-form formula for the global smoothness indicators. The authors also assessed the dominance of the parameters p and ϵ to retain the desired order of accuracy. The parameter p is set up in the formulation of nonlinear weights to ascertain that these nonlinear weights converge to the ideal weights at a fast enough convergence rate.

The convergence analysis of WENO-JS scheme explored by Arandiga et al. [1] is based on the value of ϵ , proposed that ϵ value is proportional to the square of mesh size Δx , instead of a constant value so that the scheme achieves $(2r-1)^{th}$ order of accuracy at smooth regions regardless of neighboring extrema, while this is of order r when the function has a discontinuity in the stencil of $(2r-1)$ points and is smooth in at least one of the r -point stencil. A question about the behavior of WENO-Z scheme when the ϵ value is taken in accordance with the value mentioned in [1], is examined by Don and Borges [5]. The authors made the accuracy analysis of the WENO-Z scheme and suggested a condition on the value of ϵ to achieve the full global-order of accuracy as similar to that of [1]. Further the authors have shown that the numerical oscillations can be attenuated by increasing the parameter p value from 2 to $r-1$.

An alternate to the smoothness indicators of fifth order WENO-JS scheme were formulated by Fan et al. [6] with the help of Lagrange interpolation polynomials, accordingly a very high order schemes were derived by Fan in [7]. These schemes are based on the idea of constructing higher order global smoothness indicators, due to which less dissipation occurs in the solution near discontinuities. Very recently, another version of a smoothness indicators were proposed by Ha et al. [11], measured in L_1 -norm, hereafter referred as WENO-NS scheme. The authors introduced a higher-order approximation to the first derivative in the formation of local smoothness indicators which yields an improved behavior relative to other fifth-order WENO schemes. The global smoothness indicator for the WENO-NS scheme is preferred as an average of the two measurements, the smoothness information of the five point stencil and the middle three point stencil.

Kim et al. [20] perceived that, the three sub-stencils of the fifth-order WENO-NS scheme provides an unbalanced contribution to the flux at an evaluation point along the interface and an additional contribution term which measures the smoothness of the middle stencil in the formation of global smoothness indicator. The authors made a balanced tradeoff among the sub-stencils through a parameter δ and a global smoothness indicator is figured out which doesn't depend on the smoothness information of the middle three point stencil anymore. These modifications lead to better results than the WENO-NS as well as other fifth-order WENO schemes, this scheme is pointed out as WENO-P scheme in the later part of this article.

A simple analysis verifies that the WENO-NS and WENO-P schemes attain the fifth-order accuracy at first order critical points but fails to achieve the accuracy at the points where second derivative vanishes. We have suggested a modified WENO-P scheme in [24] based on the idea of the linear combination of second-order derivatives, leading to a higher-order derivative information, is used in the construction of a global smoothness indicator. The modified smoothness indicator satisfies the sufficient condition, assert the requirement to achieve desired order of accuracy, even in the case of second order derivative vanishes.

In this article, a seventh order WENO scheme is derived in the lines of [11] and [24]. The smoothness indicators are obtained from the generalized undivided difference operator. Each of this operator is up to fourth-order of accuracy at the evaluation point, so the resulting scheme is seventh order accurate. Introduced parameters ξ_1, ξ_2 to balance the tradeoff between the accuracies around the smooth to the discontinuous regions. The global smoothness indicator so earned satisfies the sufficient condition to get the optimal order of convergence rate, unvarying in the presence of critical points. Utilized strong stability preserving Runge-Kutta schemes introduced in [10] to advance the time. These are detailed out in the following sections, briefly they are:

Section 2, deals with the preliminaries about WENO reconstruction to the one-dimensional scalar conservation laws and section 3 introduces the proposed WENO scheme where a new global measurement and local smoothness indicators are derived, which estimates the smoothness of a local solution in the construction of a seventh-order WENO scheme. Numerics for one-dimensional scalar test problems such as linear advection, Burger's equation, the examples pertaining to the system of Euler equations such as shock tube problems, 1D shock-entropy wave interaction problem and 2D Riemann problem of gas dynamics are reported in Section 4, to demonstrate the advantages of the proposed WENO scheme. Finally, concluding remarks are in Section 5.

2 The fundamentals of WENO scheme

This part accounts to the construction of the seventh order weighted essentially non-oscillatory scheme in a finite difference framework for approximate the solution of hyperbolic conservation laws

$$u_t + f(u)_x = 0, \quad x \in (-\infty, \infty), \quad t \in (0, \infty), \quad (1)$$

with initial condition

$$u(x, 0) = u_0(x), \quad x \in (-\infty, \infty). \quad (2)$$

Here $u = (u_1, u_2, \dots, u_m)^T$ is a m -dimensional vector of conserved variables defined for space and time variables x and t respectively, f is a flux function which depends on the conserved quantity u . The system (1) is called hyperbolic if all the eigen values $\lambda_1, \lambda_2, \dots, \lambda_m$ of the Jacobian matrix $A = \frac{\partial f}{\partial u}$ of the flux function are real and the set of right eigen vectors are complete.

For numerical approximation the spatial domain is discretized with uniform grid, for brevity in the presentation. Let $\Delta x = x_{j+\frac{1}{2}} - x_{j-\frac{1}{2}}$ be the length of the j^{th} cell $I_j = [x_{j-\frac{1}{2}}, x_{j+\frac{1}{2}}]$ with center $x_j = \frac{1}{2}(x_{j+\frac{1}{2}} + x_{j-\frac{1}{2}})$, here $x_{j\pm\frac{1}{2}}$ are known as cell interfaces. The approximation of the spatial derivative in the hyperbolic conservation laws (1) yields a semi-discrete formulation

$$\frac{du_j}{dt} = -\frac{1}{\Delta x} (\hat{f}_{j+\frac{1}{2}} - \hat{f}_{j-\frac{1}{2}}). \quad (3)$$

Here u_j is an approximation to u at a point $x = x_j$ in time t , i.e., for the value $u(x_j, t)$ and $\hat{f}_{j\pm\frac{1}{2}}$ are the numerical fluxes which are Lipschitz continuous in each of its arguments and are consistent with the physical flux, that means $\hat{f}(u, \dots, u) = f(u)$. The conservation property is retrieved by defining a function h implicitly through the equation (see Lemma 2.1 of [32])

$$f(x) := f(u(x, \cdot)) = \frac{1}{\Delta x} \int_{x-\frac{\Delta x}{2}}^{x+\frac{\Delta x}{2}} h(\xi) d\xi. \quad (4)$$

Differentiating (4) with respect to x yields

$$f(u(x, \cdot))_x = \frac{1}{\Delta x} \left(h \left(x + \frac{\Delta x}{2} \right) - h \left(x - \frac{\Delta x}{2} \right) \right),$$

thus $h(x \pm \frac{\Delta x}{2})$ should be an approximation to the numerical flux $\hat{f}_{j\pm\frac{1}{2}}$, such that

$$\hat{f}_{j\pm\frac{1}{2}} = h \left(x_{j\pm\frac{1}{2}} \right) + O(\Delta x^{2r-1}),$$

r represents the number of cells in a stencil. Thus the numerical flux $\hat{f}_{j\pm\frac{1}{2}}$ can be acquired by using higher order polynomial interpolation to $h(x_{j\pm\frac{1}{2}})$ with the help of known values of $f(x)$ at the cell centers, $f_j = f(x_j)$.

To ensure the numerical stability and to avoid entropy violating solutions, the flux $f(u)$ is splitted into two parts f^+ and f^- , the positive and negative parts of $f(u)$ respectively, such that

$$f(u) = f^+(u) + f^-(u), \quad (5)$$

where $\frac{df^+(u)}{du} \geq 0$ and $\frac{df^-(u)}{du} \leq 0$. The numerical fluxes \hat{f}^+ and \hat{f}^- evaluated at $x = x_{j+\frac{1}{2}}$ reduces (5) as

$$\hat{f}_{j+\frac{1}{2}} = \hat{f}_{j+\frac{1}{2}}^+ + \hat{f}_{j+\frac{1}{2}}^-.$$

We will describe here how $\hat{f}_{j+\frac{1}{2}}^+$ can be approximated, as $\hat{f}_{j+\frac{1}{2}}^-$ is symmetric to the positive part with respect to $x_{j+\frac{1}{2}}$. In the description for the approximation of $\hat{f}_{j+\frac{1}{2}}^+$ to follow we drop the '+' sign in the superscript, for simplicity.

2.1 Seventh order WENO scheme

WENO scheme prefers $(2r - 1)$ points global stencil, S^{2r-1} , to achieve $(2r - 1)^{th}$ order of accuracy. The stencil S^{2r-1} is subdivided into r sub-stencils with each sub-stencil bearing r cells. In particular, seventh-order WENO scheme accounts to a 7-points stencil, which is subdivided into four 4-points sub-stencils S^0, S^1, S^2, S^3 . In accordance with cell I_j , each sub-stencil encloses four grid points, specified as

$$S^k(j) = \{x_{j+k-3}, x_{j+k-2}, x_{j+k-1}, x_{j+k}\}, k = 0, 1, 2, 3.$$

A third degree interpolating polynomial $\hat{f}^k(x)$ is formulated in each sub-stencil $S^k(j)$ and evaluating it at the cell boundary $x_{j+\frac{1}{2}}$, we retain

$$\hat{f}^k\left(x_{j+\frac{1}{2}}\right) = \hat{f}_{j+\frac{1}{2}}^k = \sum_{q=0}^3 c_{k,q} f_{j+k-3+q}, \quad (6)$$

where the coefficients $c_{k,q}$ ($q = 0, 1, 2, 3$) are the Lagrange interpolation coefficients, independent of the values of the flux function f , but depends on the left shift parameter $k = 0, 1, 2, 3$. The equation (6) on each stencil takes the form

$$\begin{aligned} \hat{f}_{j+\frac{1}{2}}^0 &= -\frac{1}{4}f_{j-3} + \frac{13}{12}f_{j-2} - \frac{23}{12}f_{j-1} + \frac{25}{12}f_j, \\ \hat{f}_{j+\frac{1}{2}}^1 &= \frac{1}{12}f_{j-2} - \frac{5}{12}f_{j-1} + \frac{13}{12}f_j + \frac{1}{4}f_{j+1}, \\ \hat{f}_{j+\frac{1}{2}}^2 &= -\frac{1}{12}f_{j-1} + \frac{7}{12}f_j + \frac{7}{12}f_{j+1} - \frac{1}{12}f_{j+2}, \\ \hat{f}_{j+\frac{1}{2}}^3 &= \frac{1}{4}f_j + \frac{13}{12}f_{j+1} - \frac{5}{12}f_{j+2} + \frac{1}{12}f_{j+3}. \end{aligned}$$

The fluxes $\hat{f}_{j-\frac{1}{2}}^k$ can be fetched through shifting the index to the left by one in (6). The Taylor's expansion of the fluxes $\hat{f}_{j\pm\frac{1}{2}}^k$, settle in as

$$\hat{f}_{j\pm\frac{1}{2}}^k = h_{j\pm\frac{1}{2}} + A_4^k f_j^{(4)} \Delta x^4 + O(\Delta x^5),$$

where A_4^k is the leading order coefficient in the expansion and $f_j^{(4)}$ is the 4th derivative of $f(x)$ at $x = x_j$. The convex combination of these flux functions leads to the approximation of $\hat{f}_{j+\frac{1}{2}}$, that is, we set

$$\hat{f}_{j+\frac{1}{2}} = \sum_{k=0}^3 \omega_k \hat{f}_{j+\frac{1}{2}}^k. \quad (7)$$

Here ω_k 's are non-linear weights, satisfying the conditions

$$\omega_k \geq 0, k = 0, 1, 2, 3 \text{ and } \sum_{k=0}^3 \omega_k = 1.$$

If the function $h(x)$ is free from discontinuities in all of the sub-stencils $S^k(j)$, $k = 0, 1, 2, 3$, we can assess the constants d_k such that the linear combination of $\hat{f}_{j\pm\frac{1}{2}}^k$ provides the seventh order convergence to $\hat{f}_{j\pm\frac{1}{2}}$, that is,

$$\hat{f}_{j\pm\frac{1}{2}} = \sum_{k=0}^3 d_k \hat{f}_{j\pm\frac{1}{2}}^k = h_{j\pm\frac{1}{2}} + A_7 f_j^{(7)} \Delta x^7 + O(\Delta x^8).$$

The d_k 's are termed as the ideal weights since they invokes the upstream central scheme of seventh-order, in seven points stencil. The values of these ideal weights are evaluated as

$$d_0 = 1/35, d_1 = 12/35, d_2 = 18/35, d_3 = 4/35. \quad (8)$$

When the non-linear weights ω_k are equal to the ideal weights d_k , we have

$$\frac{1}{\Delta x} \left(\hat{f}_{j+\frac{1}{2}} - \hat{f}_{j-\frac{1}{2}} \right) = \frac{1}{\Delta x} \left(\left(h_{j+\frac{1}{2}} - h_{j-\frac{1}{2}} \right) + O(\Delta x^8) \right) = f'(x_j) + O(\Delta x^7),$$

thus the approximation to the spatial derivative of the flux $f(x)$ at the cell-centre $x = x_j$ is $O(\Delta x^7)$. Hence the sufficient condition to achieve the seventh order convergence for the scheme is given by

$$\omega_k^{\sim} - d_k = O(\Delta x^4) \quad (9)$$

where the superscripts \sim and $-$ on ω_k corresponds to their use in either $\hat{f}_{j+\frac{1}{2}}^k$ and $\hat{f}_{j-\frac{1}{2}}^k$ respectively. Note that the condition (9) can be weakened for WENO-JS scheme to $\omega_k^{\sim} - d_k = g\left(x_{j+\frac{1}{2}}\right) (\Delta x^3) + O(\Delta x^4)$ for a locally Lipschitz continuous function g under a suitable condition, which depends on the value of ϵ .

3 The numerical scheme, WENO-NS7

The essential ingredient of the WENO schemes is in the computation of smoothness indicators, Ha et. al. [11] have established the smoothness indicators measured in L_1 -norm for the fifth-order WENO scheme. Here we are extending it to the higher order schemes, particularly for the seventh order WENO scheme and calling the scheme as WENO-NS7. The primary thought is of getting a higher order approximation to the derivatives, as it is known that a smoothness indicators based on L_1 -norm may give a loss of accuracy in smooth regions [26]. The heuristic construction of smoothness indicators is as follows.

Define the operators $L_{s,k}f$ which measures the regularity of the solution in each of the four points stencil $S^k(j) = \{x_{j+k-3}, x_{j+k-2}, x_{j+k-1}, x_{j+k}\}$, $k = 0, 1, 2, 3$ by estimating the approximate magnitude of derivatives. Once obtained these operators, the smoothness indicators β_k are designed as

$$\beta_k = \xi_1 |L_{1,k}f| + \xi_2 |L_{2,k}f| + |L_{3,k}f|, \quad (10)$$

here $\xi_i \in (0, 1]$, $i = 1, 2$, are the parameters introduced to balance the tradeoff between the accuracy around the smooth region to that of the discontinuous region. The operators $L_{s,k}f$ are the generalized undivided differences of f , which are formulated as

$$L_{s,k}f \left(x_{j+\frac{1}{2}} \right) := \sum_{x_l \in S^k(j)} c_{k,l}^{[s]} f(x_l), \quad s = 1, 2, 3, \quad (11)$$

where the coefficient vector

$$c_k^{[s]} := \left(c_{k,l}^{[s]} : x_l \in S^k(j) \right)^T, \quad s = 1, 2, 3, \quad (12)$$

is obtained by solving the linear system

$$\sum_{x_l \in S^k(j)} c_{k,l}^{[s]} \frac{\left(x_l - x_{j+\frac{1}{2}} \right)^m}{m!} = \begin{cases} \Delta x^s, & \text{if } s = m, \\ 0, & \text{if } s \neq m. \end{cases}$$

with $m = 0, 1, 2, 3$. This linear system can be written in the matrix form

$$M c_k^{[s]} = r,$$

with the matrices M and r defined by

$$M = M_{k,j} := \left(\frac{\left(x_l - x_{j+\frac{1}{2}} \right)^m}{m!} : x_l \in S_k(j), m = 0, 1, 2, 3 \right),$$

$$r = r_s := \left(\Delta x^s \delta_{s,m} : m = 0, 1, 2, 3 \right)^T,$$

where $\delta_{s,m}$ is the Kronecker delta and there exist a unique solution for this linear system, as M is a Vandermode matrix. With the coefficients (12) the operators (11) takes the form

$$\begin{aligned} L_{1,0}f &= \frac{1}{24}(-23f_{j-3} + 93f_{j-2} - 141f_{j-1} + 71f_j), \quad L_{2,0}f = \frac{1}{2}(-3f_{j-3} + 11f_{j-2} - 13f_{j-1} + 5f_j), \\ L_{1,1}f &= \frac{1}{24}(f_{j-2} - 3f_{j-1} - 21f_j + 23f_{j+1}), \quad L_{2,1}f = \frac{1}{2}(-3f_{j-2} + 5f_{j-1} - 7f_j + 3f_{j+1}), \\ L_{1,2}f &= \frac{1}{24}(f_{j-1} - 27f_j + 27f_{j+1} - f_{j+2}), \quad L_{2,2}f = \frac{1}{2}(f_{j-1} - f_j - f_{j+1} + f_{j+2}), \\ L_{1,3}f &= \frac{1}{24}(-23f_j + 21f_{j+1} + 3f_{j+2} - f_{j+3}), \quad L_{2,3}f = \frac{1}{2}(3f_j - 7f_{j+1} + 5f_{j+2} - f_{j+3}), \end{aligned}$$

$$\begin{aligned} L_{3,0}f &= (-f_{j-3} + 3f_{j-2} - 3f_{j-1} + f_j), \\ L_{3,1}f &= (-f_{j-2} + 3f_{j-1} - 3f_j + f_{j+1}), \\ L_{3,2}f &= (-f_{j-1} + 3f_j - 3f_{j+1} + f_{j+2}), \\ L_{3,3}f &= (-f_j + 3f_{j+1} - 3f_{j+2} + f_{j+3}). \end{aligned}$$

The third operator $L_{3,k}f$ is the same as in the WENO-BS scheme which is described in appendix. However WENO-NS7 scheme uses the absolute values where as the WENO-BS uses the squared ones. The advantages with these operators $L_{s,k}f$ is that the approximation of the derivative

$\Delta x^s f^{(s)}$ to be of higher order accuracy at the evaluation point, $x_{j+\frac{1}{2}}$, which is stated in the following theorem.

Theorem Let the stencil $S^k(j) = \{x_{j+k-3}, x_{j+k-2}, x_{j+k-1}, x_{j+k}\}$, $k = 0, 1, 2, 3$, and assume that $f \in C^4(I)$ where I is an open interval containing $S_k(j)$. For each $s = 1, 2, 3$, the operator (11) satisfies

$$L_{s,k}f(x_{j+\frac{1}{2}}) = \frac{d^s f}{dx^s} \Delta x^s + O(\Delta x^4).$$

proof The proof follows in a similar lines that of the Theorem 3.2 of [11]. The Taylor's expansion of the operators $L_{s,k}f$ for each s and k reveals

$$\begin{aligned} L_{1,0}f &= \Delta x f_{j+\frac{1}{2}}^{(1)} - \frac{22}{24} \Delta x^4 f_{j+\frac{1}{2}}^{(4)} + O(\Delta x^5), & L_{2,0}f &= \Delta x^2 f_{j+\frac{1}{2}}^{(2)} - \frac{43}{24} \Delta x^4 f_{j+\frac{1}{2}}^{(4)} + O(\Delta x^5), \\ L_{1,1}f &= \Delta x f_{j+\frac{1}{2}}^{(1)} + \frac{1}{24} \Delta x^4 f_{j+\frac{1}{2}}^{(4)} + O(\Delta x^5), & L_{2,1}f &= \Delta x^2 f_{j+\frac{1}{2}}^{(2)} - \frac{7}{24} \Delta x^4 f_{j+\frac{1}{2}}^{(4)} + O(\Delta x^5), \\ L_{1,2}f &= \Delta x f_{j+\frac{1}{2}}^{(1)} + O(\Delta x^5), & L_{2,2}f &= \Delta x^2 f_{j+\frac{1}{2}}^{(2)} + \frac{5}{24} \Delta x^4 f_{j+\frac{1}{2}}^{(4)} + O(\Delta x^5), \\ L_{1,3}f &= \Delta x f_{j+\frac{1}{2}}^{(1)} - \frac{1}{24} \Delta x^4 f_{j+\frac{1}{2}}^{(4)} + O(\Delta x^5), & L_{2,3}f &= \Delta x^2 f_{j+\frac{1}{2}}^{(2)} - \frac{7}{24} \Delta x^4 f_{j+\frac{1}{2}}^{(4)} + O(\Delta x^5), \end{aligned}$$

$$\begin{aligned} L_{3,0}f &= \Delta x^3 f_{j+\frac{1}{2}}^{(3)} - 2\Delta x^4 f_{j+\frac{1}{2}}^{(4)} + O(\Delta x^5), \\ L_{3,1}f &= \Delta x^3 f_{j+\frac{1}{2}}^{(3)} - \Delta x^4 f_{j+\frac{1}{2}}^{(4)} + O(\Delta x^5), \\ L_{3,2}f &= \Delta x^3 f_{j+\frac{1}{2}}^{(3)} + O(\Delta x^5), \\ L_{3,3}f &= \Delta x^3 f_{j+\frac{1}{2}}^{(3)} - \Delta x^4 f_{j+\frac{1}{2}}^{(4)} + O(\Delta x^5). \end{aligned}$$

Thus the operators are in tuned with the Theorem 3.1 stated above.

Now the non-linear weights for the scheme are defined as

$$\omega_k^{NS7} = \frac{\alpha_k^{NS7}}{\sum_{q=0}^3 \alpha_q^{NS7}}, \quad \alpha_k^{NS7} = d_k \left(1 + \frac{\zeta}{(\beta_k + \epsilon)^2} \right), \quad k = 0, 1, 2, 3, \quad (13)$$

where ζ , a global smoothness indicator is taken as

$$\zeta = |\beta_0 - \beta_3|^2, \quad (14)$$

and d_k the ideal weights, given in (8). To avoid the scenario of zero division a small number $0 < \epsilon \ll 1$ is incorporated in the calculations of non-linear weights (13).

Next we discuss the convergence analysis of the WENO-NS7 scheme, in-particularly at the critical points, i.e., we analyze how the weights ω_k^{NS7} approaches to the ideal weights d_k in the presence of critical points.

3.1 Convergence order of WENO-NS7 scheme

First consider that there are no critical points and let's take $\epsilon = 0$ in (10), from Taylor's series expansion

$$\beta_k = \xi_1 \left| \Delta x f_{j+\frac{1}{2}}^{(1)} \right| + \xi_2 \left| \Delta x^2 f_{j+\frac{1}{2}}^{(2)} \right| + \left| \Delta x^3 f_{j+\frac{1}{2}}^{(3)} \right| + O(\Delta x^4) \quad \text{for all } k. \quad (15)$$

Similarly from the expansion of the global smoothness indicator (14), we've

$$\zeta = \left[\frac{81}{24} \Delta x^4 f_{j+\frac{1}{2}}^{(4)} + O(\Delta x^5) \right]^2. \quad (16)$$

Then there exist a constant D such that

$$\begin{aligned} 1 + \frac{\zeta}{\beta_k^2} &= 1 + D\Delta x^6 + O(\Delta x^7), \\ &= (1 + D\Delta x^6) \left(1 + \frac{O(\Delta x^7)}{1 + D\Delta x^6} \right), \\ &= D_{\Delta x} (1 + O(\Delta x^7)), \end{aligned} \quad (17)$$

where $D_{\Delta x} = (1 + D\Delta x^6) > 0$.

If $f_{j+\frac{1}{2}}^{(1)} = 0$, $f_{j+\frac{1}{2}}^{(2)} \neq 0$, from (15) the smoothness indicators are of the form

$$\beta_k = \left| \Delta x^2 f_{j+\frac{1}{2}}^{(2)} \right| (1 + O(\Delta x)),$$

then there exists a constant D_1 such that

$$\begin{aligned} 1 + \frac{\zeta}{\beta_k^2} &= 1 + D_1\Delta x^4 + O(\Delta x^5), \\ &= (1 + D_1\Delta x^4) \left(1 + \frac{O(\Delta x^5)}{1 + D_1\Delta x^4} \right), \\ &= D_{\Delta x}^1 (1 + O(\Delta x^5)), \end{aligned} \quad (18)$$

where $D_{\Delta x}^1 = (1 + D_1\Delta x^4) > 0$. Similarly if $f_{j+\frac{1}{2}}^{(1)} = 0$, $f_{j+\frac{1}{2}}^{(2)} = 0$, $f_{j+\frac{1}{2}}^{(3)} \neq 0$, then there exist a constant D_2 such that

$$1 + \frac{\zeta}{\beta_k^2} = 1 + D_2\Delta x^2 + O(\Delta x^3). \quad (19)$$

From (17) and (18), the weights ω_k^{NS7} satisfies the sufficient condition (9) if the first derivative vanishes but not the second derivative. In order to satisfy the sufficient condition even at higher order critical points, the nonlinear weights are defined as

$$\omega_k^{NS7} = \frac{\alpha_k^{NS7}}{\sum_{q=0}^3 \alpha_q^{NS7}}, \quad \alpha_k^{NS7} = d_k \left[1 + \left(\frac{\zeta}{(\beta_k + \epsilon)^2} \right)^s \right], \quad k = 0, 1, 2, 3, \quad (20)$$

where s can be chosen such that the sufficient condition have to hold. Note that from the expansions given in (15-19) and from (20) we have

$$\omega_k^{NS7} = \begin{cases} d_k + O(\Delta x^6)^s, & \text{if } f_{j+\frac{1}{2}}^{(1)} \neq 0, \\ d_k + O(\Delta x^4)^s, & \text{if } f_{j+\frac{1}{2}}^{(1)} = 0, f_{j+\frac{1}{2}}^{(2)} \neq 0, \\ d_k + O(\Delta x^2)^s, & \text{if } f_{j+\frac{1}{2}}^{(1)} = 0, f_{j+\frac{1}{2}}^{(2)} = 0, f_{j+\frac{1}{2}}^{(3)} \neq 0. \end{cases}$$

Clearly, the sufficient condition (9) is satisfies for the WENO-NS7 scheme under the following conditions:

1. $s \geq 1$ if $f_{j+\frac{1}{2}}^{(1)} \neq 0$, or if $f_{j+\frac{1}{2}}^{(1)} = 0$ and $f_{j+\frac{1}{2}}^{(2)} \neq 0$.
2. $s \geq 2$ if $f_{j+\frac{1}{2}}^{(1)} = 0$, $f_{j+\frac{1}{2}}^{(2)} = 0$, $f_{j+\frac{1}{2}}^{(3)} \neq 0$.

For numerical verification, s value is taken as 2. With these developments, in the next section we'll test the WENO-NS7 scheme for various examples.

4 Numerical results

Let's denote the system (1) by

$$\frac{du}{dt} = L(u),$$

where $L(u)$ is an approximation to the derivative $-f(u)_x$. In section 2, we have obtained higher order reconstruction for the flux function which is defined in (3). To evolve the solution in time, strong-stability-preserving Runge–Kutta (*SSPRK*) algorithm is used, whose detailed description is in article [10]. The choice of this time integration is to ensure that the order of accuracy for the time evaluation matches with that of the spatial order of accuracy. For linear problems, m -stage linear *SSPRK* method, which is of $(m - 1)^{th}$ order is used in the following examples. The *lSSPRK*($m, m - 1$) method is

$$\begin{aligned} u^{(0)} &= u^n, \\ u^{(i)} &= u^{(i-1)} + \frac{1}{2}\Delta t L(u^{(i-1)}), i = 1, \dots, m - 1 \\ u^{(m)} &= u^{n+1} = \sum_{k=0}^{m-2} \alpha_{m,k} u^{(k)} + \alpha_{m,m-1} \left(u^{(m-1)} + \frac{1}{2}\Delta t L(u^{(m-1)}) \right). \end{aligned}$$

For the seventh order the coefficients $\alpha_{m,k}$, ($m = 8$) are given as

$$\alpha_{8,0} = \frac{2}{15}, \alpha_{8,1} = \frac{2}{7}, \alpha_{8,2} = \frac{2}{9}, \alpha_{8,3} = \frac{4}{15}, \alpha_{8,4} = 0, \alpha_{8,5} = \frac{4}{45}, \alpha_{8,6} = 0, \alpha_{8,7} = \frac{1}{315}.$$

This method will not attain $O(\Delta t^m)$ for nonlinear problems. So, for nonlinear problems a fourth order nonlinear version of *SSPRK*(5,4) is used with the stability condition $CFL \leq 1$, where $CFL = \max_j \{S_j^n \frac{\Delta t}{\Delta x}\}$. Here S_j^n is the maximum propagation speed in I_j at time level t^n . The fourth order *SSPRK*(5,4) method is given as

$$\begin{aligned} u^{(1)} &= u^n + 0.39175222\Delta t L(u^n), \\ u^{(2)} &= 0.444370494\Delta u^n + 0.5556295u^{(1)} + 0.36841059\Delta t L(u^{(1)}), \\ u^{(3)} &= 0.62010185\Delta u^n + 0.379898u^{(2)} + 0.25189177\Delta t L(u^{(2)}), \\ u^{(4)} &= 0.17807995u^n + 0.82192004u^{(3)} + 0.5449747\Delta t L(u^{(3)}), \\ u^{n+1} &= 0.517231u^{(2)} + 0.0960597u^{(3)} + 0.3867086u^{(4)} + 0.063692\Delta t L(u^{(3)}) + 0.22600748\Delta t L(u^{(4)}). \end{aligned}$$

For numerical comparison of the proposed WENO-NS7 scheme, the numerical results are presented along with the numerical results of seventh order WENO-BS [2] and seventh order WENO-Z [5] schemes in the following sections. These results are mostly comparable with WENO-BS scheme in compare to other seventh-order WENO schemes. For completeness these schemes are briefly described in the appendix.

4.1 Scalar test problems

To verify the numerical accuracy and convergence of the scheme examples pertaining to transport and Burger's equations with various initial profiles are considered. Some of these initial profiles contain jump discontinuity and in some cases, the solution in time leads to shocks. Lax-Friedrich's flux splitting technique is used in (5). For the scheme WENO-BS, $\epsilon = 10^{-6}$ and for WENO-Z and WENO-NS7 schemes $\epsilon = 10^{-40}$ is taken along with the CFL number 0.5. The parameters in (10) are fixed as $\xi_1 = 0.1$ and $\xi_2 = 1$ for linear test cases.

4.1.1 Behaviors of new weights

Example 1: For linear advection equation

$$u_t + u_x = 0, -1 \leq x \leq 1, t > 0,$$

let the initial condition be

$$u(x, 0) = u_0(x) = \begin{cases} -\sin(\pi x) - \frac{1}{2}x^3 & \text{for } -1 \leq x < 0, \\ -\sin(\pi x) - \frac{1}{2}x^3 + 1 & \text{for } 0 \leq x < 1, \end{cases} \quad (21)$$

which is a piecewise continuous function with jump discontinuity at $x = 0$. The behavior of the smoothness indicators β_k ($k = 0, 1, 2, 3$) and the global smoothness indicator ζ for initial time, $t = 0$ is displayed in figure 1 for the proposed scheme WENO-NS7.

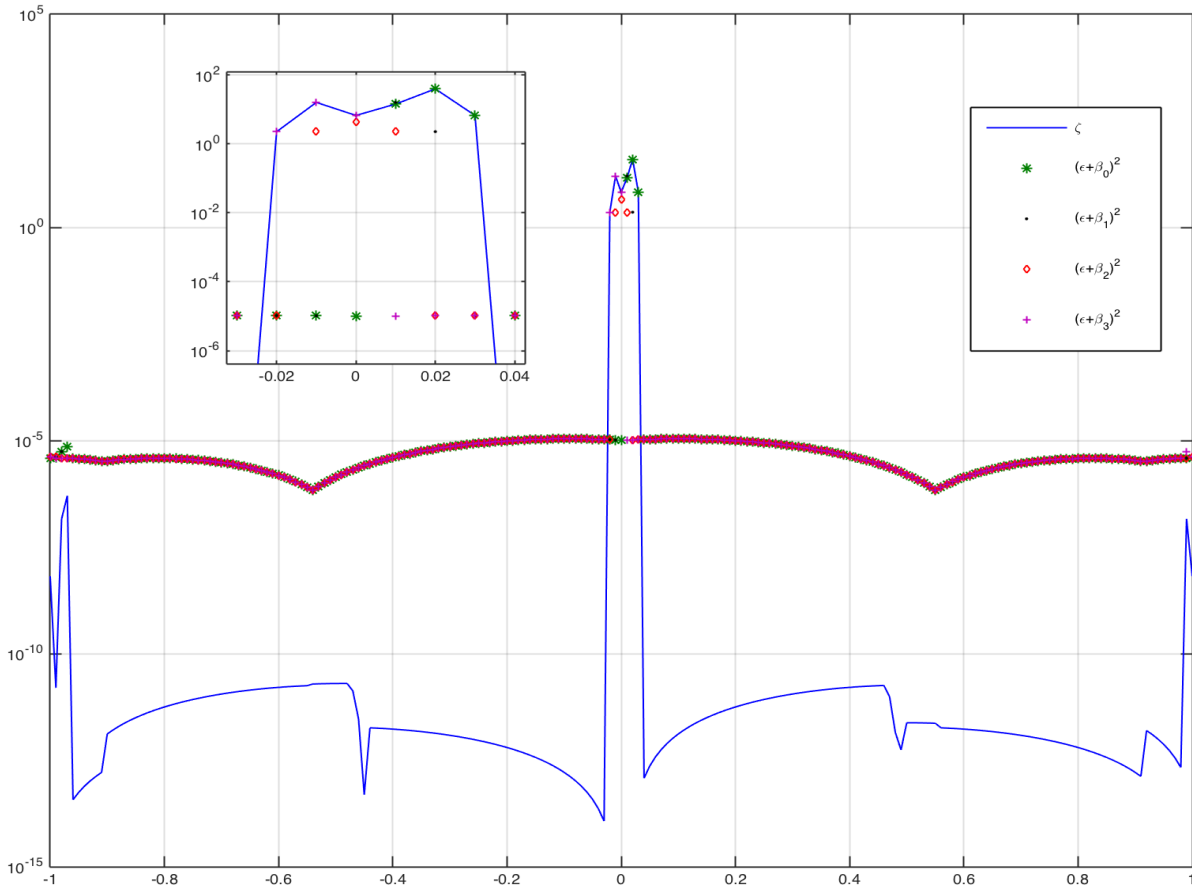


Figure 1: The values of the smoothness indicators β_k to initial data (21) by WENO-NS7 scheme

The approximate solution is computed with uniform discretization of the spatial domain with the step size, $\Delta x = 0.01$ up to time $t = 8$ with the scheme WENO-NS7 along with WENO-BS and WENO-Z schemes, these solutions are plotted in figure 2 against the exact solution. It can be observed from the plot that the proposed scheme performs better than other schemes near the jump discontinuity. Figure 3 displays the behavior of the weights ω_k along with the ideal weights d_k .

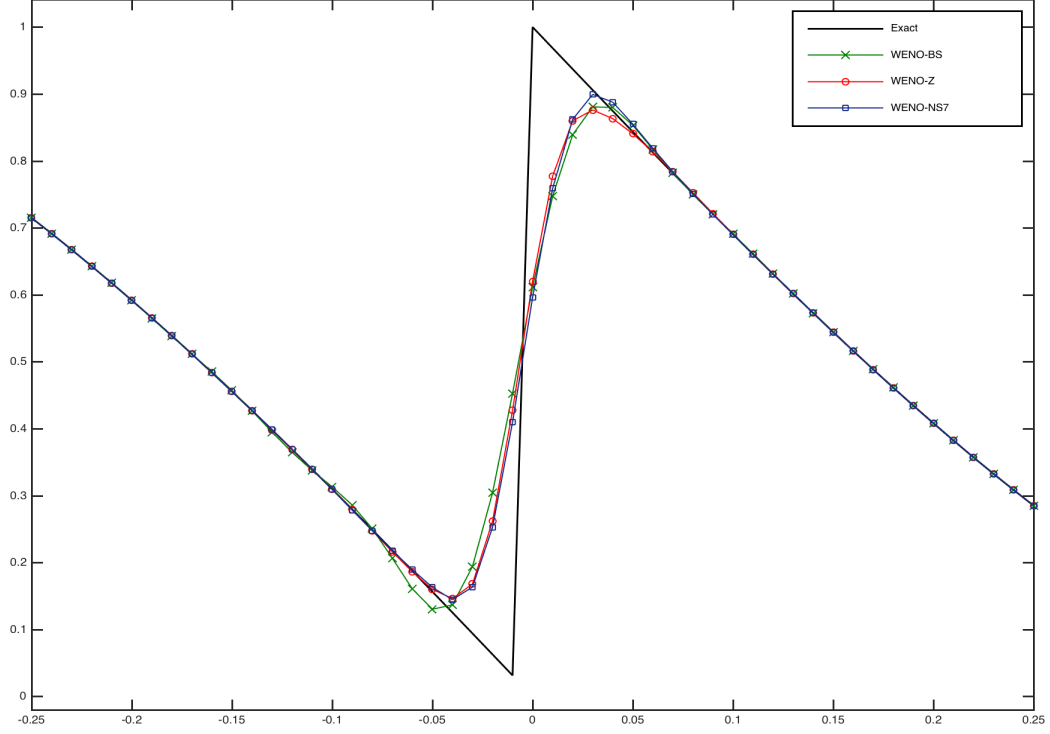


Figure 2: Numerical solution of linear advection equation with the initial condition (21)

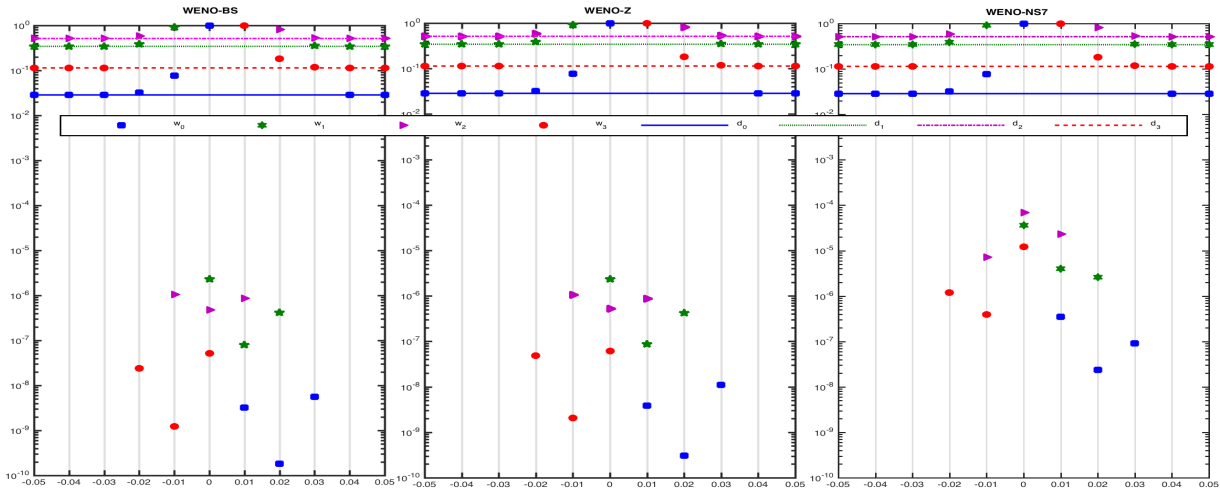


Figure 3: The distribution of ideal weights d_k and the weights $\omega_k, k = 0, 1, 2, 3$.

4.1.2 Accuracy, at critical points

Example 2: Consider the linear transport equation

$$u_t + u_x = 0, \quad -1 \leq x \leq 1, \quad t > 0, \quad (22)$$

with the periodic boundary conditions up to time $t = 2$. Three different initial conditions are considered, each of them is a special case to test the convergence analysis.

Case 1: The smooth initial condition

$$u(x, 0) = \sin(\pi x), \quad (23)$$

is taken in this case to verify the order of convergence.

In table 1, the L_1 and L_∞ errors along with the numerical order of accuracy are given for WENO-BS, WENO-Z and WENO-NS7 schemes. It has been observed that the proposed scheme attains the desired order of accuracy and very much efficient than WENO-BS scheme but has the same accuracy as WENO-Z scheme.

N	WENO-BS		WENO-Z		WENO-NS7	
	L_1 error	L_1 order	L_1 error	L_1 order	L_1 error	L_1 order
10	3.9281e-03	—	6.5177e-04	—	9.9734e-04	—
20	8.5335e-05	5.52	4.2296e-06	7.26	5.6871e-06	7.45
40	1.2222e-06	6.12	3.3547e-08	6.98	3.3551e-08	7.40
80	1.8418e-08	6.05	2.6304e-10	6.99	2.6304e-10	6.99
160	2.7931e-10	6.04	2.0638e-12	6.99	2.0637e-12	6.99
N	L_∞ error		L_∞ error		L_∞ error	
	L_∞ error	L_∞ order	L_∞ error	L_∞ order	L_∞ error	L_∞ order
10	8.5830e-03	—	1.4372e-03	—	2.0586e-03	—
20	2.2095e-04	5.28	6.7946e-06	7.72	1.5028e-05	7.09
40	5.3163e-06	5.38	5.2546e-08	7.01	6.8261e-08	7.78
80	1.4576e-07	5.18	4.1283e-10	6.99	4.3546e-10	7.29
160	4.0863e-09	5.15	3.2415e-12	6.99	3.2736e-12	7.05

Table 1: L_1 and L_∞ – errors of example (22) with initial condition (23)

Case 2: In this case, the initial condition is chosen as

$$u(x, 0) = \sin(\pi x - \frac{1}{\pi} \sin(\pi x)), \quad (24)$$

which contains first-order critical point, that is, $u_x = 0$ but note that $u_{xxx} \neq 0$.

The L_1 and L_∞ errors along with the numerical order of accuracy are provided in table 2 for WENO-BS, WENO-Z and WENO-NS7 schemes. The proposed scheme WENO-NS7 achieves the desired order of accuracy.

Case 3: The initial condition

$$u(x, 0) = \sin(\pi x)^3, \quad (25)$$

has the nature, $u_x = 0$, $u_{xx} = 0$ but $u_{xxx} \neq 0$.

In table 3, the L_1 and L_∞ errors are tabulated along with the numerical order of accuracy for the schemes WENO-BS, WENO-Z and WENO-NS7. In this case too, the proposed scheme has the desired order of convergence.

	WENO-BS		WENO-Z		WENO-NS7	
N	L_1 error	L_1 order	L_1 error	L_1 order	L_1 error	L_1 order
10	2.9823e-02	—	3.0006e-02	—	1.3986e-02	—
20	7.5922e-04	5.29	5.0945e-04	5.88	3.0947e-04	5.49
40	8.3317e-06	6.51	2.6348e-06	7.59	2.6567e-06	6.86
80	6.9845e-08	6.89	2.1488e-08	6.93	2.1524e-08	6.94
160	7.1684e-10	6.60	1.6933e-10	6.99	1.6934e-10	6.99
	L_∞ error	L_∞ order	L_∞ error	L_∞ order	L_∞ error	L_∞ order
10	7.1325e-02	—	7.0754e-02	—	3.6883e-02	—
20	2.2429e-03	4.99	1.3617e-03	5.70	9.2089e-04	5.32
40	3.6731e-05	5.93	7.9578e-06	7.41	7.9697e-06	6.85
80	5.8755e-07	5.96	6.6439e-08	6.90	6.6272e-08	6.91
160	1.1019e-08	5.73	5.2713e-10	6.97	5.2711e-10	6.97

Table 2: L_1 and L_∞ — errors of example (22) with initial condition (24)

	WENO-BS		WENO-Z		WENO-NS7	
N	L_1 error	L_1 order	L_1 error	L_1 order	L_1 error	L_1 order
10	2.1618e-01	—	2.1128e-01	—	1.9695e-01	—
20	1.8858e-02	3.52	8.4032e-03	4.65	8.6604e-03	4.50
40	4.1300e-04	5.51	6.4354e-05	7.02	8.6452e-05	6.64
80	5.9000e-06	6.13	4.2948e-07	7.22	4.1937e-07	7.68
160	6.6306e-08	6.47	3.3639e-09	6.99	3.3582e-09	6.96
	L_∞ error	L_∞ order	L_∞ error	L_∞ order	L_∞ error	L_∞ order
10	2.9623e-01	—	2.9814e-01	—	3.2319e-01	—
20	3.8372e-02	2.95	1.4710e-02	4.34	1.7309e-02	4.22
40	1.0319e-03	5.21	1.4691e-04	6.64	2.1456e-04	6.33
80	2.3364e-05	5.46	6.6758e-07	7.78	1.0238e-06	7.71
160	6.1191e-07	5.25	5.2805e-09	6.98	5.5897e-09	7.51

Table 3: L_1 and L_∞ — errors of example (22) with initial condition (25)

Example 3: Consider the linear advection equation $u_t + u_x = 0$ on an interval $[-1, 1]$ with the initial condition

$$u(x, 0) = \begin{cases} \frac{1}{6}[G(x, z - \delta) + G(x, z + \delta) + 4G(x, z)], & -0.8 \leq x \leq -0.6 \\ 1, & -0.4 \leq x \leq -0.2 \\ 1 - |10(x - 0.1)|, & 0 \leq x \leq 0.2 \\ \frac{1}{6}[F(x, a - \delta) + F(x, a + \delta) + 4F(x, a)], & 0.4 \leq x \leq 0.6 \\ 0, & \text{otherwise} \end{cases} \quad (26)$$

where $G(x, z) = \exp(-\beta(x - z)^2)$, $F(x, a) = \{\max(1 - \alpha^2(x - a)^2, 0)\}^{\frac{1}{2}}$, $a = 0.5$, $z = -0.7$, $\delta = 0.005$, $\alpha = 10$ and $\beta = \left(\frac{\log(2)}{36\delta^2}\right)$. This initial condition consists of several shapes that contains the combination of Gaussian, a square wave, a sharp triangle wave and an half ellipse, which are difficult to resolve by the numerical schemes, so it turns out to be a typical test case for numerical verification. The solution is computed with periodic boundary conditions on the mesh of 200 cells up to time $t = 8$ by the schemes WENO-NS7, WENO-BS and WENO-Z. These solutions are

plotted in figure 4 against the exact solution, from the figure one can observe that WENO-NS7 scheme performs better than WENO-BS and WENO-Z schemes.

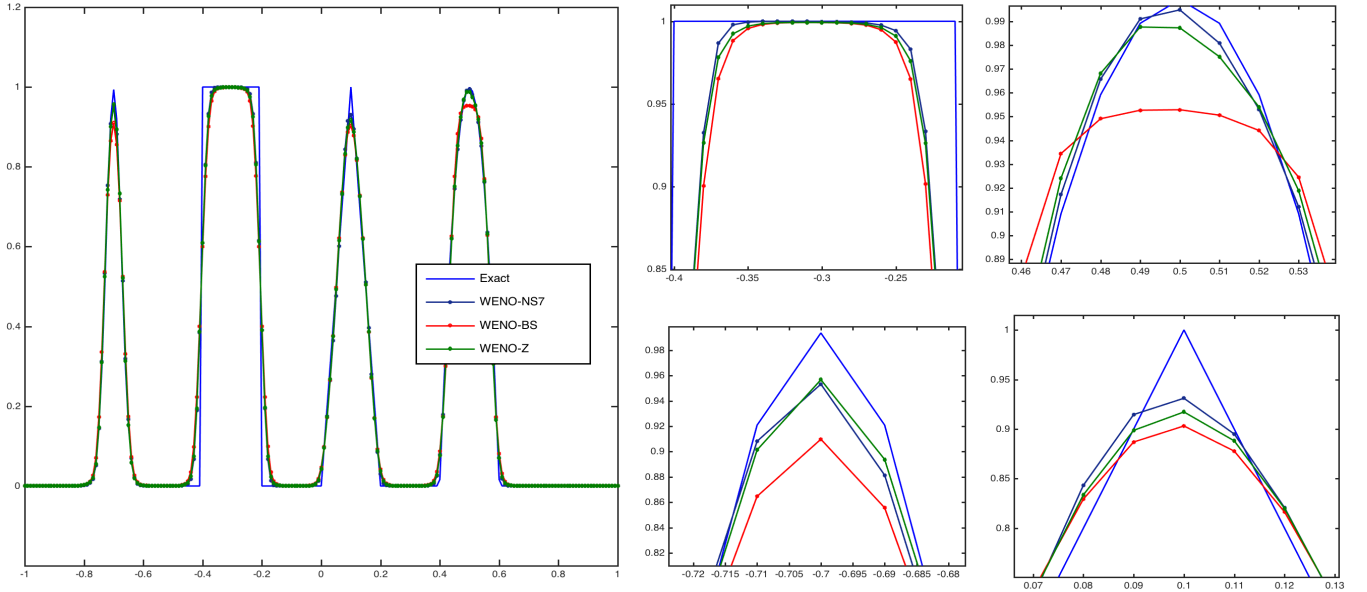


Figure 4: Numerical solution of linear advection equation with the initial condition (26)

4.1.3 Test with shocks

Example 4: Consider the inviscid Burger's equation

$$u_t + \left(\frac{u^2}{2}\right)_x = 0, \quad -1 \leq x \leq 1, \quad t > 0, \quad (27)$$

with the following initial conditions.

Case 1: The initial condition

$$u_0(x) = -\sin(\pi x), \quad (28)$$

produces a steady shock at the point $x = 0$ as the time progresses from $t = 0$ to $t = 1.5$.

The numerical solution is computed with the periodic boundary conditions, on the mesh of 200 grid cells. The approximate solutions are plotted in figure 5 against the reference (exact) solution. It is noted from this figure that the WENO-NS7 scheme captures the shock very well in compare WENO-BS and WENO-Z schemes.

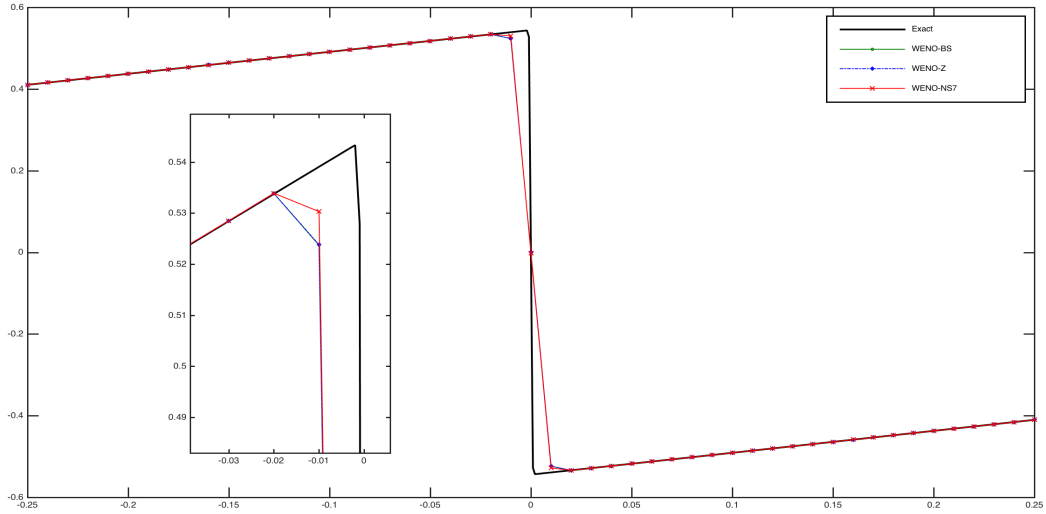


Figure 5: Approximate solution of (27) with initial condition (28) and its zoomed region.

Case 2: Consider the initial condition

$$u_0(x) = \frac{1}{2} + \sin(\pi x), \quad (29)$$

for the equation (27), which generates a moving shock-wave at time $t = 0.55$. The numerical results for the WENO-NS7 along with the WENO-BS and WENO-Z schemes are plotted in the figure 6 on the computational grid of 200 cells against the reference solution. Here too, WENO-NS7 scheme captures the shock better than other schemes.

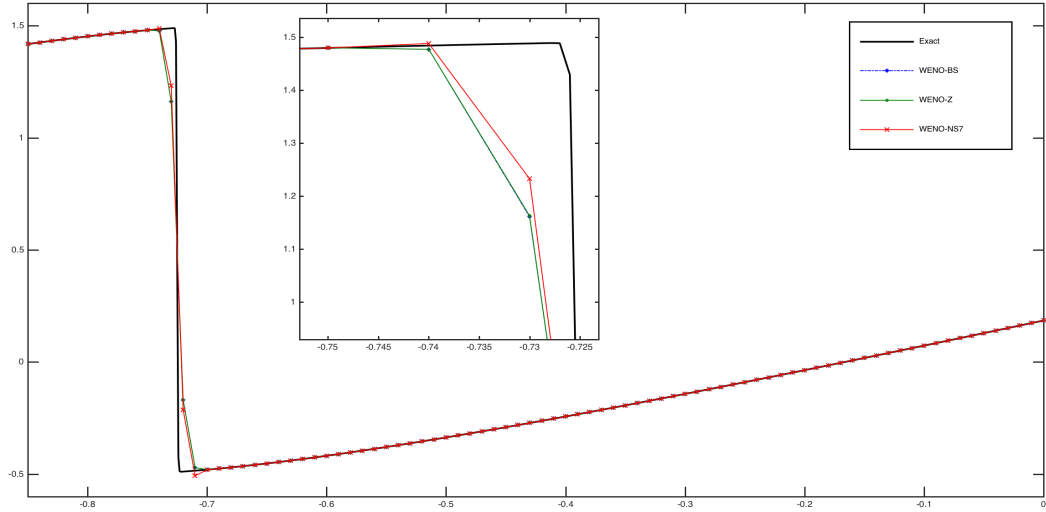


Figure 6: Approximate solution of (27) with initial condition (29) and its zoomed region.

Remark We've chosen the parameters $\xi_1 = 0.1$ and $\xi_2 = 0.3$ to evaluate the equation (10) for the solution of (27).

4.2 Euler equations in one space dimension

The one-dimensional system of Euler equations are given by

$$\begin{pmatrix} \rho \\ \rho u \\ E \end{pmatrix}_t + \begin{pmatrix} \rho u \\ \rho u^2 + p \\ u(E + p) \end{pmatrix}_x = 0 \quad (30)$$

where ρ, u, E, p are the density, velocity, total energy and pressure respectively.

The system (30) represents the conservation of mass, momentum and total energy. The total energy for an ideal polytropic gas is defined as

$$E = \frac{p}{\gamma - 1} + \frac{1}{2}\rho u^2, \quad (31)$$

where γ is the ratio of specific heats and its value is taken as $\gamma = 1.4$.

For the numerical evaluation of this system by WENO-NS7 scheme, in the following examples the parameters in (5) are taken as $\xi_1 = 0.3$ and $\xi_2 = 0.3$.

4.2.1 Shock tube problems

Consider the system (30) with the following well-known initial conditions:

Example 5: The Riemann data

$$(\rho, u, p) = \begin{cases} (1.0, 0.75, 1.0), & \text{if } 0 \leq x \leq 0.5, \\ (0.125, 0.0, 0.1), & \text{if } 0.5 \leq x \leq 1, \end{cases} \quad (32)$$

is a modified version of Sod's shock tube problem [33], its solution contains a right shock wave, a right traveling contact wave and a left sonic rarefaction wave. The numerical results are obtained on a grid of 200 cells for the spatial domain $0 \leq x \leq 1$ up to $t = 0.2$ with the transmissive boundary conditions. The density, pressure and velocity profiles are plotted in figures 7, 8 and 9 respectively, against the reference solution and the diagrams contain the enlarged portions of shock and contact discontinuity regions. From these figures, one can conclude that WENO-NS7 scheme performs better in compare to WENO-BS and WENO-Z schemes.

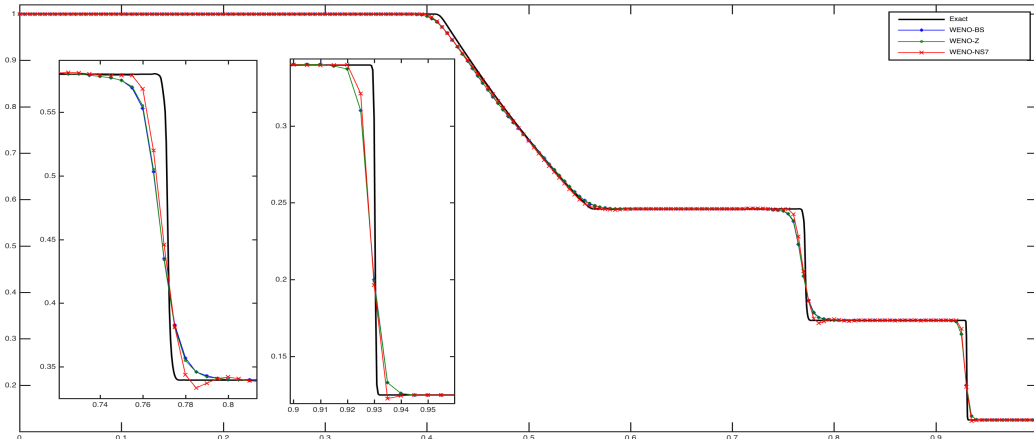


Figure 7: Density profile for Sod's shock tube problem.

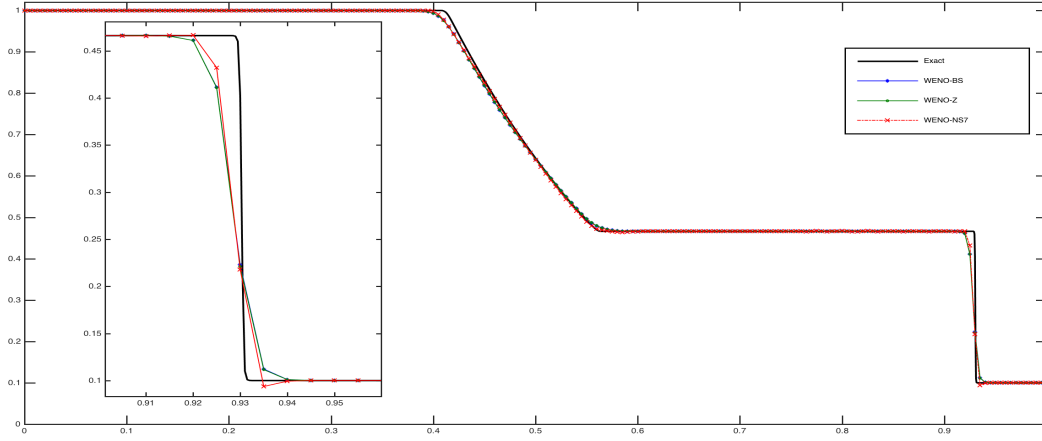


Figure 8: Pressure profile of Sod's shock tube problem.

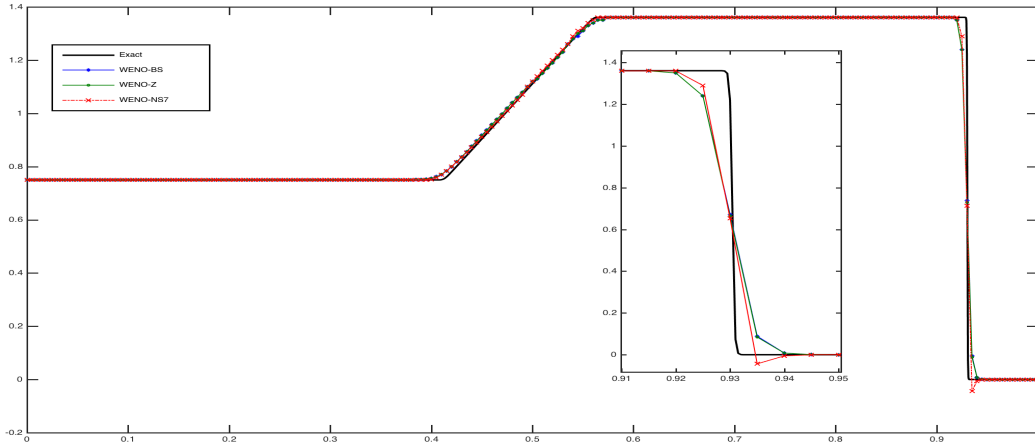


Figure 9: Velocity profile of Sod's shock tube problem.

Example 6: The initial condition

$$(\rho, u, p) = \begin{cases} (0.445, 0.698, 3.528), & \text{if } -5 \leq x < 0, \\ (0.500, 0.000, 0.571), & \text{if } 0 \leq x \leq 5, \end{cases} \quad (33)$$

is due to Lax [21]. This problem reveals the shock capturing capabilities of the numerical scheme.

The numerical solutions are computed on the computational domain $-5 \leq x \leq 5$ with 200 grid cells up to time $t = 1.3$. Figures 10, 11 and 12 displays that the density, pressure and velocity profiles against the reference solution. WENO-NS7 performs better in this case too.

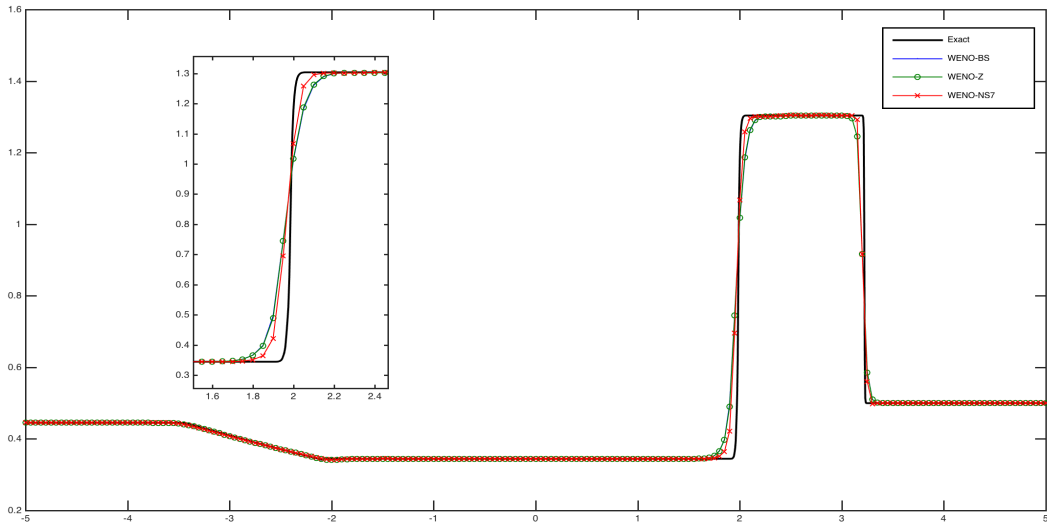


Figure 10: Density profile for Lax initial condition.

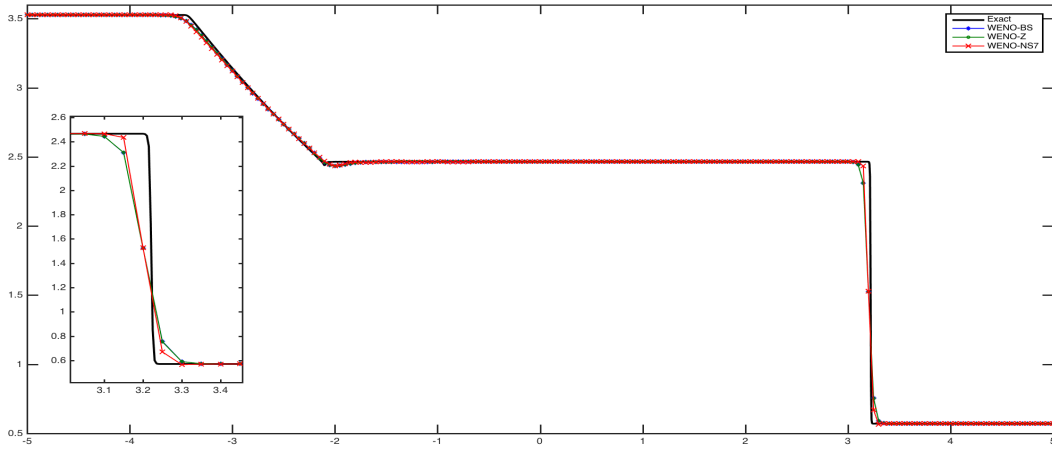


Figure 11: Pressure profile for Lax initial condition.

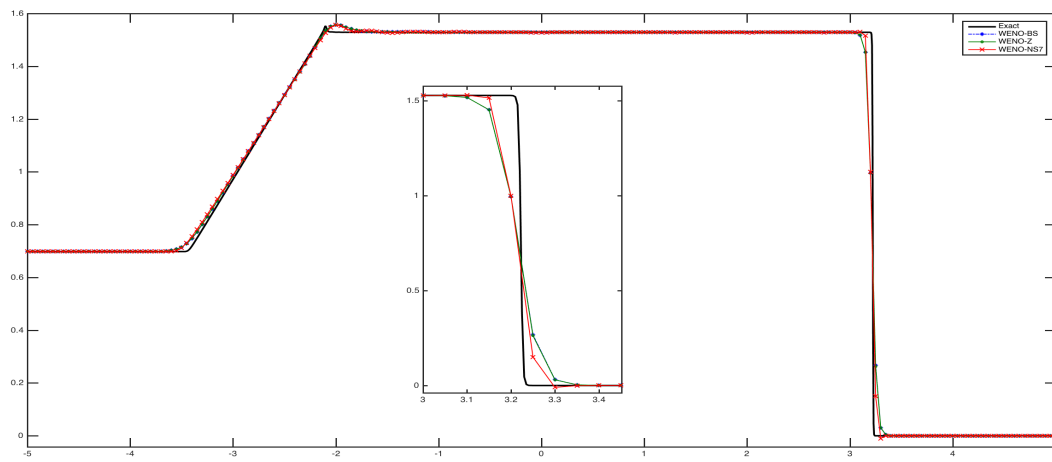


Figure 12: Velocity profile for Lax initial condition.

4.2.2 1D shock entropy wave interaction problem

Example 7: Consider the system (30) on the spatial domain $x \in [-5, 5]$, with the Riemann data

$$(\rho, u, p) = \begin{cases} (3.857143, 2.629369, 10.33333), & \text{if } -5 \leq x < -4, \\ (1 + \epsilon \sin(kx), 0.000, 1.000), & \text{if } -4 \leq x \leq 5. \end{cases} \quad (34)$$

where ϵ and k are the amplitude and wave number of the entropy wave respectively, chosen as $\epsilon = 0.2$ and $k = 5$. This problem is known as shock entropy wave interaction problem [34], the solution has a right-moving supersonic (Mach 3) shock wave which interacts with sine waves in a density disturbance that generates a flow field with both smooth structures and discontinuities. This flow induces wave trails behind a right-going shock with wave numbers higher than the initial density-variation wave number k . The initial condition contains a jump discontinuity at $x = -4$, especially the initial density profile has oscillations on $[-4, 5]$.

The numerical results are computed with 200 and 400 spatial grid points up to time $t = 1.8$, the results are plotted against the reference solution in figures 13 and 14 respectively. The proposed scheme WENO-NS7 performs better than other seventh order schemes, which can be observed from these figures.

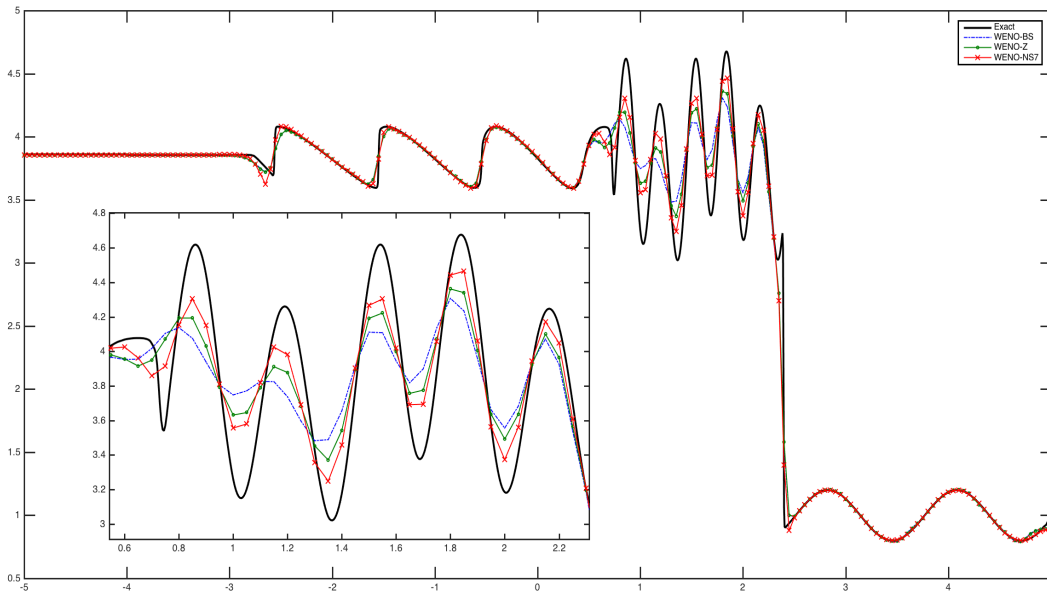


Figure 13: Shock entropy wave interaction test with 200 grid points

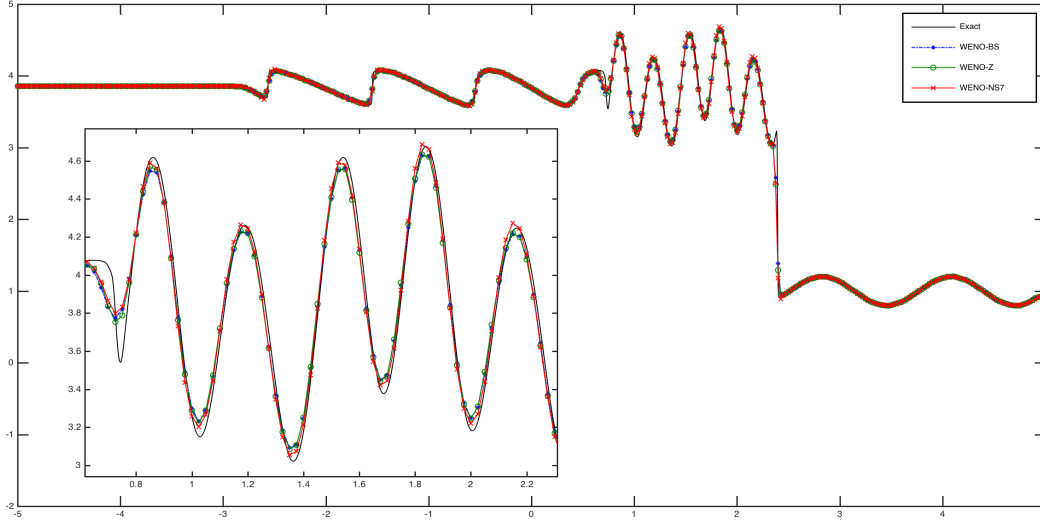


Figure 14: Shock entropy wave interaction test with 400 points

4.3 Two-Dimensional Euler equations

In this section, we apply the proposed scheme to two-dimensional problem in cartesian coordinates. The governing two-dimensional compressible Euler equations are given by

$$U_t + F(U)_x + G(U)_y = 0, \quad (35)$$

where

$$U = (\rho, \rho u, \rho v, E)^T, \quad F(U) = (\rho u, P + \rho u^2, \rho uv, u(E + P))^T, \quad G(U) = (\rho v, \rho uv, P + \rho v^2, v(E + P))^T.$$

Here ρ, u, v are density, x -velocity component and y -velocity component respectively.

The total energy E can be obtained from the equation

$$p = (\gamma - 1)\left(E - \frac{1}{2}\rho(u^2 + v^2)\right),$$

where p is the pressure and γ is the ratio of specific heats.

Example 8: For the PDE (35) on the domain $[0, 1] \times [0, 1]$, consider the initial condition

$$(\rho, u, v, p) = \begin{cases} (1.5, 0, 0, 1.5) & \text{if } 0.8 \leq x \leq 1, 0.8 \leq y \leq 1, \\ (0.5323, 1.206, 0, 0.3) & \text{if } 0 \leq x < 0.8, 0.8 \leq y \leq 1, \\ (0.138, 1.206, 1.206, 0.029) & \text{if } 0 \leq x < 0.8, 0 \leq y < 0.8, \\ (0.5323, 0, 1.206, 0.3) & \text{if } 0.8 < x \leq 1, 0 \leq y \leq 0.8, \end{cases}$$

given by Rinne et. al. in [25], here each quadrant is divided by lines $x = 0.8$ and $y = 0.8$. This initial condition produce a narrow jet by the merge of four shocks. The numerical solution is computed on the mesh of 400×400 grid points up to time $t = 0.8$ with Dirichlet boundary conditions and is displayed in figure 15. An examination of this result reveal that WENO-NS7 yields a better solution of the complex structure when compares to WENO-BS and WENO-Z schemes.

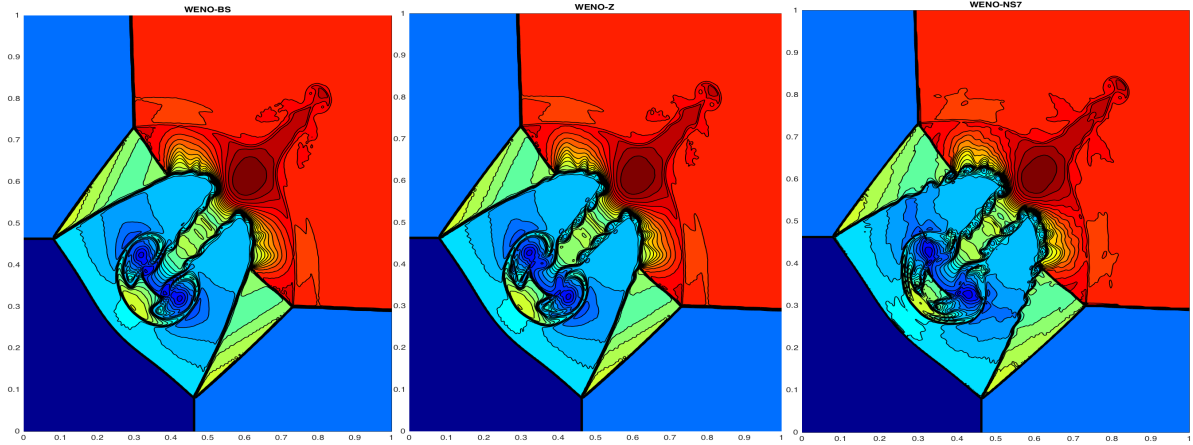


Figure 15: Density profiles of 2D problem with the mesh $\Delta x = \Delta y = 1/400$

5 Conclusions

In this article, a new seventh-order weighted essentially non-oscillatory scheme is presented to approximate the solution of nonlinear hyperbolic conservation laws, named as WENO-NS7 scheme. Based on undivided differences of derivatives of an interpolation polynomials over a stencil, the local as well as global smoothness indicators are constructed, measured in L_1 -sense, to approximate the nonlinear weights. We analyzed the scheme in the presence of critical points and found that the proposed scheme possesses the desirable order of accuracy when the first and second-order derivative vanishes. The approximate solutions of the one and two-dimensional hyperbolic conservation laws are simulated with the proposed WENO-NS7 scheme and compared it with WENO-BS and WENO-Z schemes. Numerical experiments show that the proposed WENO-NS7 scheme yields better approximation in comparison to the WENO-BS and WENO-Z schemes. As a future work, working on the construction of higher order schemes (order greater than seven).

6 Appendix

For completeness, here we are describing briefly the WENO-BS and WENO-Z schemes, these schemes are used in numerical comparison.

6.1 WENO-BS

For the reconstruction of flux (7), Balsara and Shu [2] has taken the non-linear weights ω'_k s as

$$\omega_k = \frac{\alpha_k}{\sum_{q=0}^3 \alpha_q}, \alpha_k = \frac{d_k}{(\epsilon + \beta_k)^p}, k = 0, 1, 2, 3, \quad (36)$$

where $0 < \epsilon \ll 1$ is introduced to prevent $\alpha_k \rightarrow \infty$, the smoothness indicator β_k , measures the smoothness of a solution over a particular stencil and $p \geq 1$ is a parameter. The value of p is chosen such that the nonlinear weights, in non-smooth regions approaches to zero at an accelerated rate as $\Delta x \rightarrow 0$. The suggested smoothness indicators β_k are the same as that of WENO-JS [19], which

are given by

$$\beta_k = \sum_{q=1}^3 \Delta x^{2q-1} \int_{x-\frac{\Delta x}{2}}^{x+\frac{\Delta x}{2}} \left(\frac{d^q \hat{f}^k}{dx^q} \right)^2 dx. \quad (37)$$

The explicit form of these smoothness indicators are as follows:

$$\beta_0 = f_{j-3}(547f_{j-2} - 3882f_{j-2} + 4642f_{j-1} - 1854f_j) + f_{j-2}(7043f_{j-2} - 17246f_{j-1} + 7042f_j) + f_{j-1}(11003f_{j-1} - 9402f_j) + 2107f_j^2,$$

$$\beta_1 = f_{j-2}(267f_{j-2} - 1642f_{j-1} + 1602f_j - 494f_{j+1}) + f_{j-1}(2843f_{j-1} - 5966f_j + 1922f_{j+1}) + f_j(3443f_j - 2522f_{j+1}) + 547f_{j+1}^2,$$

$$\beta_2 = f_{j-1}(547f_{j-1} - 2522f_j + 1922f_{j+1} - 494f_{j+2}) + f_j(3443f_j - 5966f_{j+1} + 1602f_{j+2}) + f_{j+1}(2843f_{j+1} - 1642f_{j+2}) + 267f_{j+2}^2,$$

$$\beta_3 = f_j(2107f_j - 9402f_{j+1} + 7042f_{j+2} - 1854f_{j+3}) + f_{j+1}(11003f_{j+1} - 17246f_{j+2} + 4642f_{j+3}) + f_{j+2}(7043f_{j+2} - 3882f_{j+3}) + 547f_{j+3}^2.$$

6.2 WENO-Z

Borges et al. [3] redefined the non-linear weights of the WENO-JS scheme [19] by introducing a global smoothness indicator τ , as

$$\omega_k^z = \frac{\alpha_k^z}{\sum_{q=0}^3 \alpha_q^z}, \quad \alpha_k^z = d_k \left(1 + \left[\frac{\tau}{\beta_k + \epsilon} \right]^p \right). \quad (38)$$

The idea here is to get the nonlinear weights ω_k^z s close to the ideal weights d_k^z s, the scheme is known as WENO-Z scheme.

For the seventh order WENO-Z scheme, Castro et. al. [4] defined the global smoothness indicator as

$$\tau_7 = |\beta_0 - \beta_1 - \beta_2 + \beta_3|. \quad (39)$$

whose truncation error is $O(\Delta x^7)$ and in [5] the author's defined another global smoothness indicator

$$\tau_7 = |\beta_0 + 3\beta_1 - 3\beta_2 - \beta_3| \quad (40)$$

whose truncation error is $O(\Delta x^8)$. The numerical convergence of the WENO-Z scheme, when used with the high-order global smoothness indicator (40) achieves better order of accuracy in comparison to the use of the global smoothness indicator (39). For the numerical comparison, we've used the global smoothness indicator (40) with the nonlinear weights (38) to compute the WENO-Z scheme. The smoothness indicators β_k^z s in (39) and (40) are as in (37).

References

- [1] Arandiga, F., Baeza, A., Belda, A.M., Mulet, P.: Analysis of WENO schemes for full and global accuracy. *SIAM J. Numer. Anal.* **49**, 893-915(2011).
- [2] Balsara, D.S., Shu, C.W.: Monotonicity preserving weighted essentially non-oscillatory schemes with increasingly high order of accuracy. *J. Comput. Phys.* **160**, 405-452(2000).
- [3] Borges, R., Carmona, M., Costa, B., Don, W.S.: An improved weighted essentially non-oscillatory scheme for hyperbolic conservation laws. *J. Comput. Phys.* **227**, 3191-3211(2008).
- [4] Castro, M., Costa, B., Don, W.S.: High order weighted essentially nonoscillatory WENO-Z schemes for hyperbolic conservation laws. *J. Comput. Phys.* **230**, 766-792(2011).
- [5] Don, W.S., Borges, R.: Accuracy of the weighted essentially non-oscillatory conservative finite difference schemes. *J. Comput. Phys.* **250**, 347-372(2013).
- [6] Fan, P., Shen, Y., Tian, B., Yang, C.: A new smoothness indicator for improving the weighted essentially non-oscillatory scheme. *J. Comput. Phys.* **269**, 329-354(2014).
- [7] Fan, P.: High order weighted essentially non oscillatory WENO-schemes for hyperbolic conservation laws. *J. Comput. Phys.* **269**, 355-285(2014).
- [8] Gerolymos, G.A., Senechal, D., Vallet, I.: Very high order WENO schemes. *J. Comput. Phys.* **228**, 8481-8524(2009).
- [9] Godunov, S.K.: A finite-difference scheme for the numerical computation of discontinuous solutions of the equations of fluid dynamics. *Matthematicheskii sbornik*, **47**, 271-290(1959).
- [10] Gottlieb, S.: On high order strong stability preserving Runge–Kutta and multi- step time discretizations. *J. Sci. Comput.* **25**, 105-28(2005) .
- [11] Ha, Y., Kim, C.H., Lee, Y.J., Yoon, J.: An improved weighted essentially non-oscillatory scheme with a new smoothness indicator. *J. Comput. Phys.* **232**, 68-86(2013).
- [12] Harten, A.: High resolution schemes for hyperbolic conservation laws. *J. Comput. Phys.* **49**, 357-393(1983).
- [13] Harten, A.: On a class of high resolution total-variation-stable finite-difference schemes. *SIAM J. Numer. Anal.* **21**,1(1984).
- [14] Harten, A., Osher, S., Engquist, B., Chakravarthy, S.R.: Some results on uniformly high-order accurate essentially nonoscillatory schemes. *App. Numer. Math.* **2**, 347-377(1986).
- [15] Harten, A., Osher, S.: Uniformly high-order accurate non oscillatory schemes, I. *SIAM J. Numer. Anal.* **24**, 279-309(1987).
- [16] Harten, A., Engquist, B., Osher, S., Chakravarthy, S.R.: Uniformly high order accurate non-oscillatory schemes, III. *J. Comput. Phys.* **131**, 3-47(1997).
- [17] Henrick, A.K., Aslam, T.D., Powers, J.M.: Mapped weighted essentially non-oscillatory schemes: Achieving optimal order near critical points. *J. Comput. Phys.* **207**, 542-567(2005).

- [18] Hu, F., Wang, R., Chen, X.: A modified fifth-order WENOZ method for hyperbolic conservation laws. *J. Comput. and App. math.* **303**, 56-68(2016).
- [19] Jiang, G.S., Shu, C.W.: Efficient implementation of Weighted ENO schemes. *J. Comput. Phys.* **126**, 202-228(1996).
- [20] Kim, C.H., Ha, Y., Yoon, J.: Modified Non-linear Weights for Fifth-Order Weighted Essentially Non-oscillatory Schemes. *J. Sci. Comput.* **67**, 299-323(2016).
- [21] Lax, P.D.: Weak solutions of nonlinear hyperbolic equations and their numerical computation. *Commun. Pure Appl. Math.* **7**, 159-193(1954).
- [22] Liu, X.D., Osher, S., Chan, T.: Weighted Essentially non-oscillatory schemes. *J. Comput. Phys.* **115**, 200-212(1994).
- [23] Osher, S., Chakravarthy, S.R.: High resolution schemes and the entropy condition. *SIAM J. Numer. Anal.* **21**,5(1984).
- [24] Rathan, S., Naga Raju, G.: A modified fifth-order WENO scheme for hyperbolic conservation laws. arxiv preprint.
- [25] Schulz-Rinne, C.W., Collins, J.P., Glaz, H.M.: Numerical solution of the riemann problem for two-dimensional gas dynamics. *SIAM J. Sci. Compu.* **14**, 1394-1414(1993).
- [26] Serna, S., Marquina, A.: Power-ENO methods: a fifth-order accurate weighted power ENO method. *J. Comput. Phys.* **194**, 632-658(2004).
- [27] Shen, Y.Q., Zha, G.C.: A Robust Seventh-order WENO Scheme and Its Applications. AIAA-2008-0757(2008).
- [28] Shen, Y.Q., Zha, G.C.: Improved Seventh-Order WENO Scheme. AIAA-2010-1451(2010).
- [29] Shu, C.W.: Essentially non-oscillatory and weighted essentially non-oscillatory schemes for hyperbolic conservation laws. In *Advanced numerical approximation of nonlinear hyperbolic equations*, Lecture Notes in Mathematics, Berlin, Springer-Verlag. **1697**, 325-432 (1998).
- [30] Shu, C.W.: High order weighted essentially non oscillatory schemes for convection dominated problems. *SIAM Review.* **51**,82-126(2009).
- [31] Shu, C.W., Osher, S.: Efficient implementation of essentially non-oscillatory shock-capturing schemes. *J. Comput. Phys.* **77**, 439-471(1988).
- [32] Shu, C.W., Osher, S.: Efficient implementation of essentially non-oscillatory shock-capturing schemes II. *J. Comput. Phys.* **83**, 32-78(1989).
- [33] Sod, G.A.: A survey of several finite difference methods for systems of nonlinear hyperbolic conservation laws. *J. Comput. Phys.* **107**, 1-31(1978).
- [34] Woodward, P., Colella, P.: The numerical simulation of two-dimensional fluid flow with strong shocks. *J. Comput. Phys.* **54**, 115-173(1984).